J. Chem. Thermodynamics 218 (2026) 107681

Contents lists available at ScienceDirect

The Journal of Chemical Thermodynamics

journal homepage: www.journals.elsevier.com/the-journal-of-chemical-thermodynamics

Experimental study and thermodynamic assessment of the reciprocal system Mg^{2+}, Ca^{2+} // Cl^{-}, SO_4^{2-}

Amedeo Morsa [a,*], Elena Yazhenskikh [a], Rhys Dominic Jacob [a], Michael Müller [a], Dmitry Sergeev [a,b]

[a] Forschungszentrum Jülich GmbH, Institute of Energy Materials and Devices, Structure and Function of Materials (IMD-1), D-52425 Jülich, Germany
[b] NETZSCH-Gerätebau GmbH, D-95100 Selb, Germany

ARTICLE INFO

Keywords:
Phase change materials
Phase equilibria
Chlorides
Sulphates
Database development

ABSTRACT

This work provides a comprehensive analysis of the reciprocal system Mg^{2+}, Ca^{2+} // Cl^{-}, SO_4^{2-}, which was experimentally investigated using thermal analysis, calorimetric techniques, and structural characterisation, and thermodynamically modelled using the FactSage software. The study aimed to deepen the understanding of phase equilibria and thermodynamic behaviour within this system, with a particular focus on exploring its potential as high-temperature phase change materials (PCMs). Within the framework of the reciprocal system, the phase equilibria of the four binary systems ($MgCl_2$-$CaCl_2$, $MgSO_4$-$CaSO_4$, $MgCl_2$-$MgSO_4$, $CaCl_2$-$CaSO_4$) are presented alongside sections representing the ionic exchange reaction ($MgCl_2$-$CaSO_4$ and $CaCl_2$-$MgSO_4$). The experimental results on phase equilibria and thermodynamics of $MgCl_2$-$CaCl_2$, $MgCl_2$-$CaSO_4$ and $CaCl_2$-$MgSO_4$ systems supported the modelling work. Given the presence of the intermediate sulphate-based compound $CaMg_2(SO_4)_3$, the phase equilibria in the quasi-binary systems involving this phase and the chlorides ($MgCl_2$-$CaMg_2(SO_4)_3$ and $CaCl_2$-$CaMg_2(SO_4)_3$) were experimentally investigated. Based on all experimental findings, the Gibbs energy dataset in the reciprocal system Mg^{2+}, Ca^{2+} // Cl^{-}, SO_4^{2-} was generated and presented in this study, contributing to the development and refinement of the thermodynamic database of inorganic salts, and providing valuable insights into the phase relationships and thermochemical behaviour of the reciprocal system.

1. Introduction

The reciprocal system comprising magnesium and calcium chlorides and sulphates represents a promising chemical framework for the identification of potential Phase Change Materials (PCMs) for medium- to high-temperature Thermal Energy Storage (TES) applications [1,2]. The combination of chloride and sulphate salts offers the opportunity to tailor thermophysical properties, particularly by lowering melting temperatures through the formation of intermediate compounds or eutectic mixtures. This approach could enhance the performance and applicability of salt-based PCMs, overcoming some of the intrinsic limitations associated with the individual components. Previous studies by the authors [3,4] have laid the groundwork for the thermodynamic assessment of the reciprocal system by evaluating key binary subsystems, including $MgSO_4$-$CaSO_4$, $MgCl_2$-$MgSO_4$ and $CaCl_2$-$CaSO_4$. However, a complete and reliable prediction of phase equilibria and thermodynamic behaviour at the reciprocal system level requires the consistent assessment of all remaining subsystems. Each binary and quasi-binary system within the reciprocal system plays a crucial role in determining its overall phase stability and thermochemical properties. Therefore, a systematic investigation of the thermodynamic properties of the pure components and their binaries is essential to enable accurate modelling of the reciprocal system. Furthermore, it is well established that sulphate salts, despite their favourable thermal properties, exhibit thermal instability at elevated temperatures, undergoing decomposition to oxides before reaching their melting points [5–8]. This behaviour limits their direct application as PCMs within certain temperature ranges. Nevertheless, understanding their phase relationships and interaction with chloride salts remains critical, as the mixing of sulphates with chlorides may lead to the formation of stable intermediate phases or low-melting eutectic compositions, potentially meeting the key requirements for effective TES materials [9].

To the best of the authors' knowledge, no previous studies have investigated the reciprocal Mg^{2+}, Ca^{2+} // Cl^{-}, SO_4^{2-} system or any of its

* Corresponding author.
E-mail address: amedeo.morsa@julumni.fz-juelich.de (A. Morsa).

https://doi.org/10.1016/j.jct.2026.107681
Received 19 November 2025; Received in revised form 11 April 2026; Accepted 20 April 2026
Available online 21 April 2026

internal sections. In this context, the present work aims to provide a comprehensive thermodynamic assessment of this reciprocal system, combining new experimental data obtained from thermal and calorimetric analyses with previously available information on the binary subsystems that constitute it. The ultimate objective is to develop and optimise a reliable and robust thermodynamic database capable of accurately describing the phase equilibria and thermochemical behaviour of the system, thus supporting the identification and selection of promising PCM candidates.

2. Experimental

2.1. Samples

The starting materials employed for the preparation of the mixtures were the pure compounds $MgCl_2$ (Sigma-Aldrich, anhydrous 99.99%), $CaCl_2$ (Alfa Aesar, anhydrous 99.99%), $MgSO_4$ (VWR Chemicals, anhydrous ≥99%, metal basis) and $CaSO_4$ (Alfa Aesar, anhydrous 99.993%) (Table 1). Prior to use, all powders were subjected to a drying treatment at 150 °C under vacuum for 24 h to ensure the removal of any residual moisture. The effectiveness of this pre-treatment was supported by thermogravimetric analyses carried out below the respective melting temperatures of the pure compounds, which showed no significant mass loss, and by room-temperature XRD patterns, in which no secondary crystalline phases were detected.

Sample handling and preparation were performed exclusively inside a glove box ($O_2 < 0.5$ ppm, $H_2O < 1$ ppm) under a dry argon atmosphere to prevent contamination. The mixtures were directly assembled in platinum crucibles, following the target molar ratios, with sample masses of approximately 100 mg, using a Mettler Toledo analytical balance with a readability of 0.1 mg. In order to prevent mass losses arising from the volatilisation of chlorides and the thermal decomposition of sulphates into oxides at high temperatures [5–8], thermal analyses were carried out in platinum tubes sealed by hydrogen-oxygen flame, ensuring a closed environment in which any gaseous species remain confined and the system stabilises its own internal equilibrium.

2.2. Instruments

2.2.1. Differential thermal analysis and thermal gravimetry (DTA/TG)

DTA measurements were performed using a STA 449C Jupiter (Netzsch). The setup included a silicon carbide oven (RT-1600 °C) and a perpendicular sample holder with type S thermocouple (Pt/(Pt10Rh)).

Table 1
Sample table.

Chemical name	Source	Initial purity (supplier specification)	Pre-treatment	Analysis method
$MgCl_2$	Sigma-Aldrich	Anhydrous 99.99%	Dried at 150 °C under vacuum for 24 h	XRD; DTA/TG
$CaCl_2$	Alfa Aesar	Anhydrous 99.99%	Dried at 150 °C under vacuum for 24 h	XRD; DTA/TG
$MgSO_4$	VWR chemicals	Anhydrous ≥99%, metal basis	Dried at 150 °C under vacuum for 24 h	XRD; DTA/TG
$CaSO_4$	Alfa Aesar	Anhydrous 99.993%	Dried at 150 °C under vacuum for 24 h	XRD; DTA/TG
$CaMg_2(SO_4)_3$	Synthesised [3]	No commercial purity specification	Used as reported in [3]	HT-XRD; DTA/TG ([3])

The temperature calibration was conducted using the well-known structure and phase transitions temperatures (m: melting; s-s: solid-solid transition) of C_6H_5COOH (m: 122.5 °C), $RbNO_3$ (s-s: 164.2 °C), $KClO_4$ (s-s: 300.8 °C), Ag_2SO_4 (s-s: 462.2 °C), CsCl (s-s: 470.0 °C), K_2CrO_4 (s-s: 668.0 °C), $BaCO_3$ (s-s: 808.0 °C), K_2SO_4 (m: 1069.0 °C), and CaF_2 (m: 1418.0 °C), provided by Netzsch, in sealed platinum tubes. The maximum deviation between nominal and measured temperatures was 5 °C, corresponding to a standard uncertainty of u(T) = 2.9 °C. The thermal experiments were carried out at a constant heating and cooling rate of 5 K/min, applying three consecutive thermal cycles under a continuous flow of argon (20 mL/min). Data acquisition and evaluation of phase transition temperatures were performed using the Proteus Analysis software package (Netzsch). Consistent results were obtained from the second cycle onward, indicating good reproducibility of the thermal events. For the interpretation of the DTA curves, the onset temperature of the endothermic peak observed during heating was taken as the eutectic transformation temperature, while the maximum temperature of the subsequent endothermic peaks was used to define both the liquidus and solid-solid transition temperatures.

2.2.2. Differential scanning calorimetry (DSC)

Calorimetric measurements were performed using two distinct DSC instruments, in accordance with methodologies applied in previous studies [3,4]. Specifically, a DSC 404C Pegasus (Netzsch) equipped with a Pt furnace (operating range: RT-1500 °C) and a type S thermocouple (Pt/Pt10Rh) was employed, alongside a Calvet-type differential scanning calorimeter, model mHTC 96 (Setaram). The latter was used for internal cross-validation and for measurements requiring higher accuracy. For both calorimetric instruments, temperature calibration procedures were carried out to ensure the accuracy of the measurements. For the DSC 404C Pegasus (Netzsch), the calibration was performed using the known phase transition temperatures (m: melting; s-s: solid-solid transition) of a series of reference compounds: C_6H_5COOH (m: 122.5 °C), $RbNO_3$ (s-s: 164.2 °C), $KClO_4$ (s-s: 300.8 °C), Ag_2SO_4 (s-s: 462.2 °C), CsCl (s-s: 470.0 °C), K_2CrO_4 (s-s: 668.0 °C), $BaCO_3$ (s-s: 808.0 °C), K_2SO_4 (m: 1069.0 °C), and CaF_2 (m: 1418.0 °C). The average temperature deviation was ±2 °C (u(T) = 1.2 °C). During the measurements, approximately 30–40 mg of sample powder were placed in an alumina liner within a platinum crucible and analysed under an argon atmosphere (flow rate: 20 mL/min) with a heating rate of 10 K/min. For the Calvet-type DSC (mHTC 96, Setaram), the calibration of both temperature and enthalpy was performed using the melting points and enthalpies of high-purity metal standards reported in the Setaram calibration reference ENR7-6ET03: In (156.6 °C; 28.5 J/g), Sn (231.9 °C; 60.2 J/g), Pb (327.5 °C; 23.0 J/g), Zn (419.5 °C; 107.4 J/g), Al (660.3 °C; 401.3 J/g), and Ag (961.8 °C; 104.8 J/g). In this case, 200–300 mg of sample powder were loaded in an alumina liner placed within platinum crucibles. The thermal measurements were conducted under a helium atmosphere with a flow rate of 5 mL/min, applying a heating rate of 4 K/min. The heat capacity (C_p°, $J \bullet mol^{-1} \bullet K^{-1}$) of the studied mixtures was determined applying the three-step ratio method [10] with sapphire (α-Al_2O_3, NIST Standard Reference Material SRM720, purity 99.95%, metal basis) [11] as a reference, according to the following equation:

$$C^\circ_{p(s)} = \frac{m_r}{m_s} \bullet \frac{DSC_s - DSC_b}{DSC_r - DSC_b} \bullet C^\circ_{p(r)} \quad (1)$$

where m is the mass of the substance (g), DSC is the signal of thermopile (μV), and subscripts b, r and s stand for baseline, reference and sample respectively. Baseline and reference measurements were performed for each measured sample separately. The sapphire reference was a disc-shaped specimen of mass comparable to that of the sample mass under analysis.

2.2.3. X-ray diffractometry (XRD)

An Empyrean diffractometer from Malvern PANalytical equipped with a Cu-LFF X-ray tube (operated at 40 kV and 40 mA), BBHD mirror and a PIX-cel3D detector was used for XRD analysis. A continuous flow of synthetic air was applied during the experiment. Lattice parameters and amounts of secondary phases were determined through Rietveld refinement using the profile analysis software TOPAS version 6 from Bruker AXS. Crystal structures were obtained from the Inorganic Crystal Structure Database (ICSD). The uncertainty for molar volume was estimated to be ±0.02 cm^3/mol. XRD investigation on targeted mixtures was conducted on samples synthesised *in situ*. The stoichiometric amounts of anhydrous end-members were thoroughly mixed, ground in an agate mortar and heated up to 900 °C for 60 h in a sealed quartz ampoule. The final powder was analysed by X-ray diffraction. Under these experimental conditions, no interaction between the sample and the silica walls was detected, as confirmed by the absence of additional phases in the XRD patterns.

3. Thermodynamic modelling

3.1. Thermodynamic data of stochiometric compounds

The fundamental thermodynamic properties of the pure components considered in this study were evaluated and compiled to support the thermodynamic assessment. Specifically, the standard enthalpies of formation ($\Delta H^0_{298,f}$), standard entropies (S^0_{298}), and temperature-dependent heat capacity functions (C_p(T)) for both solid and liquid phases are summarised in Table S 1. Additionally, Table S 2 reports the phase transition temperatures and the associated enthalpy changes related to solid-solid and solid-liquid transformations of the investigated compounds. These data provided the essential input parameters for the thermodynamic modelling and optimisation discussed in the following sections.

The heat capacity C_p of stoichiometric compounds as function of temperature is described with power series in temperature [12], as shown in Eq. (2).

$$C_p = A + B \bullet T + C \bullet T^{-2} + D \bullet T^2 + E \bullet T^3 + \ldots \quad (2)$$

3.2. Thermodynamic model for solution phase

3.2.1. Liquid

In line with the methodology adopted in previous studies on related systems [3,4], the Gibbs energy of the liquid in the present assessment was described using the modified non-ideal associate species model introduced by Besmann et al. [13]. This approach has been demonstrated to be suitable for the thermodynamic modelling of complex oxide and salt melts in previous studies [3,14,15]. The choice of this model was primarily motivated by the need for consistency with the general oxide and salt thermodynamic database employed throughout this series of works. Accordingly, the liquid phase was treated as an oxide-like solution, with the pure liquid compounds defined as the fundamental solution components. To provide equal weighting of each associate species with regard to its entropic contribution in the ideal mixing term in the oxide database, each species contains a total of two non-oxygen atoms per formula unit according to the model used in Besmann et al. [13]. For magnesium chloride, calcium chloride, magnesium sulphate and calcium sulphate, this was represented by ($MgCl_2$):1.5, $MgSO_4$, ($CaCl_2$):1.5 and $CaSO_4$, respectively, meaning that each atom stoichiometry for both chlorides is divided by 1.5. This formulation guarantees consistency with the general oxide database GTOx [16]. Furthermore, binary interaction parameters between associate species were introduced and optimised to refine the Gibbs energy expression and improve the accuracy of the liquid phase description in light of the experimental data acquired in this and previous works. The expression of the molar Gibbs energy of the solution comprises three components: the reference term, representing the contribution of the pure end-members; the ideal mixing term, accounting for configurational entropy; and an excess term introduced to describe the non-ideal interactions between components:

$$G_m = \sum x_i {}^{\circ}G_i + RT \sum x_i ln x_i + \sum \sum_{i<j} x_i x_j \sum_{\nu=0} L_{ij}^{(\nu)} (x_i - x_j)^{\nu} \quad (3)$$

where x_i is the mole fraction of phase constituent i (including the associate species), ${}^{\circ}G_i$ is the molar Gibbs energy of the pure (liquid) phase constituent i and $L_{ij}^{(\nu)}$ with ν = 0, 1, 2 are the interaction coefficients between components i and j, according to the Redlich-Kister polynomial. ${}^{\circ}G_i$ and $L_{ij}^{(\nu)}$ are temperature dependent in the same way according to Eq. (4):

$${}^{\circ}G_i, L_{ij}^{(\nu)} = A + BT + CTln(T) + DT^2 + ET^3 + F/T \quad (4)$$

Generally, the optimisation process in Eq. (4) focuses primarily on the coefficients A and B.

3.2.2. Solid solution

In the present work, the solubility of alkaline earth metal chlorides is modelled using the compound energy formalism (CEF) [17], and referred to as MCl2. Accordingly, one sublattice accommodates the alkaline earth cations (Mg^{2+}, Ca^{2+}), while the other contains the chloride anion (Cl^-), and the solution phase is represented as (Mg^{2+}, Ca^{2+})$_1$(Cl^-)$_2$. The molar Gibbs energy is expressed as in Eq. (3), with the distinction that site fractions (y_i) are used instead of molar fractions (x_i), to represent the fraction of each species occupying a given sublattice, as follows:

$$G_m = y^I_{Mg^{2+}} \circ G_{MgCl_2} + y^I_{Ca^{2+}} \circ G_{CaCl_2} + RT\left(y^I_{Mg^{2+}} ln y^I_{Mg^{2+}} + y^I_{Ca^{2+}} ln y^I_{Ca^{2+}}\right) \quad (5)$$

The Gibbs energy of the solution components was adopted from the work of Chartrand et al. [18]. In this particular case, interaction parameters were not necessary.

3.2.3. Assessment of Gibbs energy parameters

The thermodynamic assessment presented in this study was conducted following a stepwise and integrated approach. It involved, first, the evaluation of the thermodynamic properties of the pure compounds, followed by the assessment of the relevant binary and quasi-binary subsystems. The Gibbs energy dataset for the $CaSO_4$-$MgSO_4$ and both $MgCl_2$-$MgSO_4$ and $CaCl_2$-$CaSO_4$ subsystems was generated in previous works by the authors [3,4], respectively, based on experimental data from own measurements and the literature data. These previous assessments are kept in the present work, and provided the necessary foundation for the final optimisation of the reciprocal system. The thermodynamic description of the reciprocal system was therefore established by coherently integrating the information derived from all the contributing subsystems, ensuring internal consistency and an accurate representation of the overall phase equilibria and thermodynamic behaviour. The binary interaction parameters ($L_{ij}^{(\nu)}$) between species in the liquid solution were optimised, namely the reciprocal interactions between $CaCl_2$-$MgSO_4$ and $CaSO_4$-$MgCl_2$, to reproduce the solid-liquid equilibria and the enthalpy in the reciprocal system. The optimisation of the selected solution parameters of Eq. (4) based on the available experimental data (including own measurements) was performed using the CALPHAD Optimizer module included in the FactSage software [19–21].

4. Experimental and modelling results

In the following section, the results obtained from the experimental investigation and the thermodynamic assessment of selected subsystems belonging to the reciprocal system under study are reported. Three binary systems ($MgCl_2$-$MgSO_4$, $CaCl_2$-$CaSO_4$, and $MgSO_4$-$CaSO_4$)

have been previously assessed by the authors [3,4]. The optimised thermodynamic properties from these assessments have already been incorporated into the thermodynamic database utilised in the present work.

4.1. $MgCl_2$-$CaCl_2$

The $MgCl_2$-$CaCl_2$ system was first experimentally investigated by Menge [22], followed by subsequent studies by Ivanov [23] and Matiašovský [24]. These studies reported the phase diagram to be a single eutectic phase diagram with solid solubility of $MgCl_2$ in $CaCl_2$ within a composition range of 10–15 mol% $MgCl_2$. In these works [22–24], the identification of solid solubilities was achieved by plotting the time of thermal arrest as a function of composition. Grjotheim et al. [25] later re-examined the phase diagram to validate the findings of earlier studies [22–24]. Their investigation employed a range of techniques, including thermal analysis, differential thermal analysis, quenching technique with microscopic and X-ray investigations of quenched samples, and high-temperature X-ray investigations. Menge [22] reported a eutectic composition of 39.1 mol% $CaCl_2$ at a temperature of 621 °C, with a solid solution of 14.7 mol% $MgCl_2$. Ivanov [23] determined a eutectic composition of 47.2 mol% $CaCl_2$ at 611 °C with a solid solution of approximately 10 mol% $MgCl_2$. Similarly, Matiašovský [24] found a eutectic at 46.7 mol% $CaCl_2$, 614 °C, and a solid solution larger than 11.5 mol% $MgCl_2$. Grjotheim et al. [25] revised these values, reporting a eutectic composition of 47.2 mol% $CaCl_2$ at 620 °C with a solid solubility of up to 17.2 mol% $MgCl_2$ in $CaCl_2$. The phase diagram was later modelled by Chartrand et al. [18] based on experimental studies [25], resulting in a eutectic temperature of 617 °C and a solubility of $MgCl_2$ in solid $CaCl_2$ of less than 18 mol% $MgCl_2$. Their optimisation was based on the activity of $MgCl_2$ in the melt obtained from electromotive force (emf) measurements conducted by Karakaya and Thompson [26] and the enthalpy of mixing of the liquid phase [27].

The present work aimed to validate the experimental data in order to perform thermodynamic modelling on all available data. Given the presence of several sources in the literature providing data for phase diagram description and their relatively good agreement of results, in this work selected mixtures were investigated by DTA in order to confirm the eutectic composition. Two mixtures in the eutectic region (46.94 and 47.42 mol% $CaCl_2$) were analysed with DTA in alumina crucibles, and seven compositions with medium-to-high $CaCl_2$ content (47.19, 72.75, 79.93, 82.89, 88.48, 89.51 and 93.11 mol% $CaCl_2$) were examined in sealed platinum tubes. The mixtures in the 80–100 mol% $CaCl_2$ composition range were examined in order to provide a further contribution to the description of the solubility of $MgCl_2$ in $CaCl_2$, in addition to Grjotheim's contribution [25]. DTA curves are displayed in Fig. 1 and the corresponding temperature transitions are listed in S 3.

4.1.1. Thermodynamic properties of the eutectic mixture

Based on the experimental results of this study, a eutectic composition of 47.19 mol% $CaCl_2$ was proposed. For the preparation of the eutectic mixture intended for DSC analysis, the pure compounds were weighed according to their stoichiometric ratios,[1] thoroughly mixed, and sealed in an evacuated quartz ampoule. The ampoule was subsequently subjected to heat treatment at 750 °C for 72 h in a furnace. After cooling, the resulting mixture was extracted from the ampoule inside a glove box and ground using an agate mortar to obtain a fine, homogeneous powder sui for calorimetric measurements. Two DSC measurements were performed on the eutectic mixture using platinum tubes closed with platinum lids in the Setaram DSC instrument. After the measurements, a mass loss less than 4 wt% was recorded, which is considered minor but may still introduce some uncertainty in the obtained results. Since the low-temperature C_p curves exhibited an unusual and non-reproducible behaviour, they were not considered in the present work. Only the thermal signals in the melting range were evaluated (Fig. S 1 and S 4), not for the determination of C_p values, but rather to provide an estimate of the enthalpy content associated with the fusion process. The melting temperature was determined to be 624 °C (897 K). The enthalpy of fusion of the eutectic mixture was determined by integrating the experimental C_p curves, yielding a value of 33.4 ± 1.0 kJ/mol. An independent determination using a calibration method resulted in a value of 32.9 ± 1.5 kJ/mol. The average value of 33.2 ± 0.8 kJ/mol is presented in this work as the experimental enthalpy of fusion of the eutectic composition of the binary system.

4.1.2. Thermodynamic assessment

In this work, the optimisation of the binary system was performed combining available literature data – specifically phase equilibria [25], activity of $MgCl_2$ at 800 °C [26] and enthalpy of mixing of the liquid at 800 °C [27] - with newly acquired experimental data. These new experimental results include the validation of selected compositions within the phase diagram and the determination of the latent enthalpy of fusion for the eutectic composition (47.19 mol% $CaCl_2$), 33.2 kJ/mol at 624 °C. To describe the solubility of $MgCl_2$ in $CaCl_2$, the sublattice model [28] was employed, as mentioned in section 3.2.2.

The newly derived Gibbs energy data are summarised in Table 3. The recalculated phase diagram, displayed in Fig. 2, identifies a eutectic composition of 47.1 mol% $CaCl_2$ at 619.1 °C, and the limited solubility of $MgCl_2$ in $CaCl_2$ is up to 17.0 mol%. Additionally, the calculated enthalpy of fusion for the eutectic mixture is 31.2 kJ/mol, consistent with the experimental value determined in this study (Fig. S2). The calculated activity of $MgCl_2$ at 800 °C and enthalpy of mixing of the liquid at 800 °C are presented in Fig. S3 and Fig. 3, respectively.

4.2. $MgCl_2$-$CaSO_4$

The $MgCl_2$-$CaSO_4$ system has been identified as thermodynamically s with respect to the ion-exchange reaction of the reciprocal system, according to the thermodynamic data in the database. As this system has not been the subject of prior studies, the present work aims to explore and elucidate its phase equilibria by means of targeted experimental analysis. Specifically, the system has been investigated using DTA, conducted in sealed platinum tubes to avoid decomposition of sulphates, which can occur at high temperatures. A series of twelve mixtures were studied by DTA, showing no weight loss up to 1250 °C. Heating and cooling curves are shown in Fig. 4. The DTA measurements revealed multiple distinct thermal events, as listed in Table S 5, clearly indicating the occurrence of several phase equilibria due to the presence of different phases and intermediate compounds in the previously assessed binary systems, specifically $MgSO_4$-$CaSO_4$ [3]. These thermal effects were observed in both heating and cooling runs, although some, particularly those related to liquidus transitions, were more clearly distinguishable during cooling. These experimental findings represent the first reported data for this reciprocal system, addressing a gap left by previous studies that did not provide such experimental evidence.

To investigate potential intermediate phases, a mixture with the composition $MgCl_2$(30.80 mol%)-$CaSO_4$(69.20 mol%) was prepared *via* a solid-state reaction. The preparation involved mixing the pure compounds, sealing them in an evacuated quartz ampoule, and heating at 900 °C for 60 h. After cooling, the mixture was ground using an agate mortar and subsequently characterised by X-ray diffraction analysis. The detailed XRD results are provided in the supplementary material (Fig. S4, Table S6).

4.2.1. Thermodynamic properties of the low-melting mixture

To further enhance the thermodynamic understanding of the studied system, a calorimetric investigation was performed on the quasi-eutectic mixture $MgCl_2$(78.34 mol%)-$CaSO_4$(21.66 mol%), which corresponds to

[1] For all calculations the molar mass M = 102.65 g/mol of the $MgCl_2$(52.81 mol%)-$CaCl_2$(47.19 mol%) mixture was used.

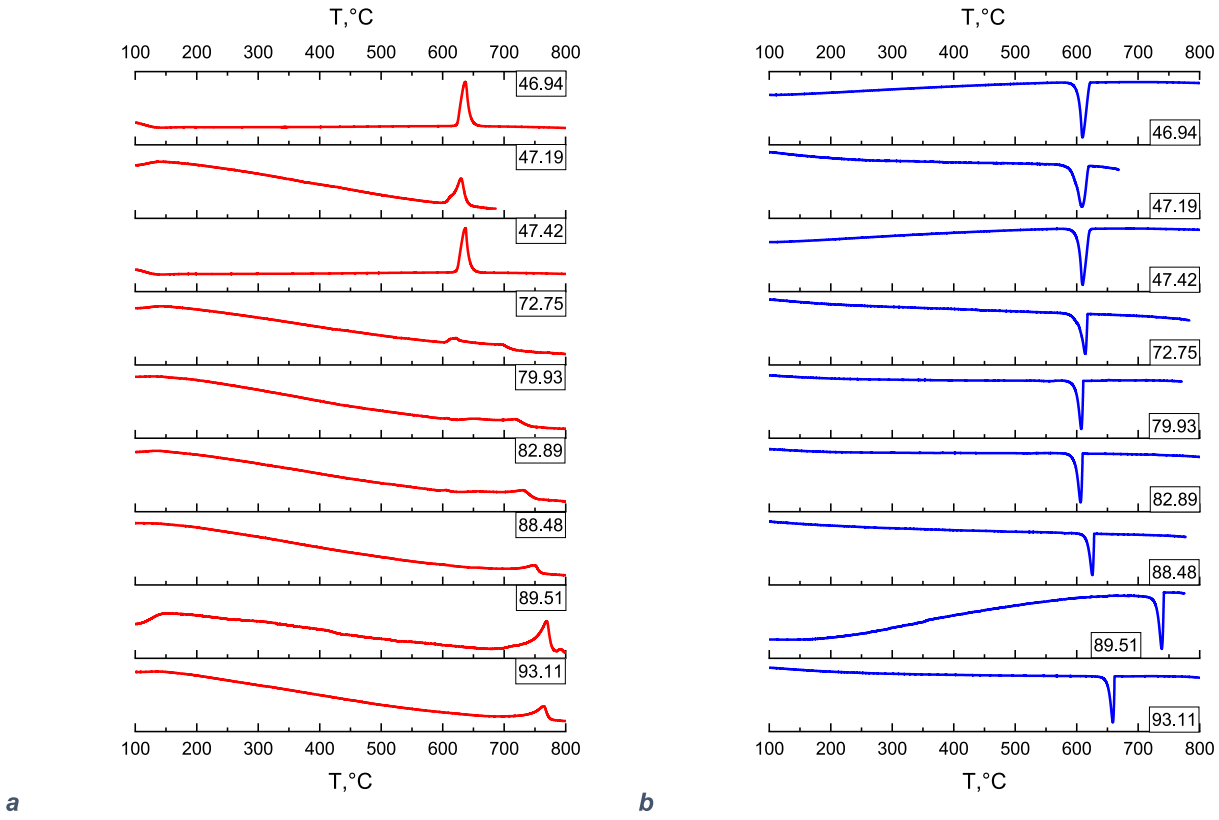

Fig. 1. DTA curves of $MgCl_2$-$CaCl_2$ mixtures, expressed in molar percentage of $CaCl_2$: **a** heating curves; **b** cooling curves.

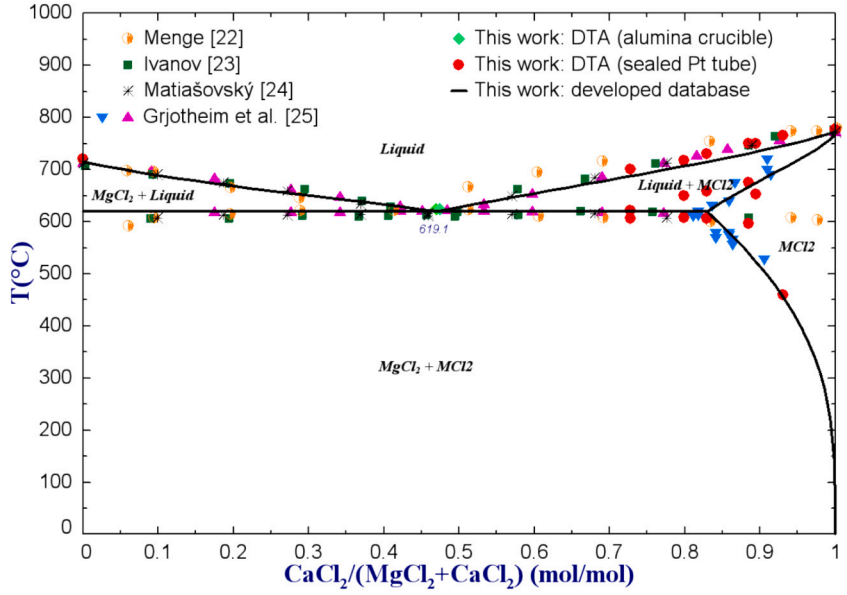

Fig. 2. Phase diagram of the $MgCl_2$-$CaCl_2$ system: comparison of experimental data obtained by DTA in the present work with experimental data from literature (Menge [22], Ivanov [23], Matiašovský [24], Grjotheim et al. [25]) and calculation with the current database.

the minimum of the liquidus line as suggested by DTA measurements. The primary goal of this analysis was to obtain additional experimental thermodynamic data, which are crucial for refining the thermodynamic model and enhancing the accuracy of the thermodynamic optimisation and database construction for the reciprocal system. Similar to the previously described mixtures, the studied mixture was prepared by mixing the pure end-members in the appropriate stoichiometric ratio.[2] The resulting mixture was sealed in an evacuated quartz ampoule and

[2] For all calculations the molar mass M = 104.08 g/mol of the $MgCl_2$(78.34 mol%)-$CaSO_4$(21.66 mol%) mixture was used.

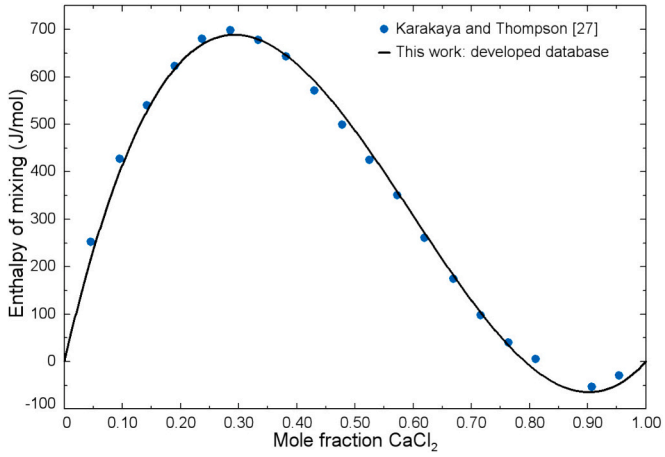

Fig. 3. Calculated enthalpy of mixing of the liquid phase at 800 °C in comparison with Karakaya and Thompson [27].

heated in a furnace at 700 °C for 48 h. After cooling, the sample was retrieved and subsequently subjected to DSC measurements. Both Netzsch and Setaram calorimeters were employed for the calorimetric measurements, and three independent samples from the same batch were analysed with each instrument. The heat capacity curves showed two distinct peaks, appearing at 591 °C (864 K) and at 632 °C (905 K), as displayed in Fig. 5 and tabulated in Table S6. The two thermal events occurred at closely spaced temperatures, and due to the experimental settings employed, they did not appear as distinctly separated peaks. Instead, the peaks partially overlapped, potentially compromising the accurate determination of enthalpy content through peak integration or area calculation. Nevertheless, a deconvolution of the overlapping peaks yielded enthalpic contributions of 13.8 kJ/mol and 19.0 kJ/mol for the first and second peaks, respectively. The calorimetric investigation of the mixture was initially aimed at identifying and characterising the thermodynamic properties of a possible eutectic composition. However, the results, together with DTA predictions, revealed that the selected composition does not correspond to an invariant eutectic point, which would have otherwise been considered a potential PCM candidate. Nevertheless, the experimental measurements provide new thermodynamic data that contribute to clarifying the behaviour of the reciprocal system and support the extension of the thermodynamic database.

4.2.2. *Thermodynamic assessment*

The thermodynamic assessment of the $MgCl_2$-$CaSO_4$ system was primarily carried out on the basis of phase transition temperatures determined by DTA measurements. The optimisation of the interaction parameters in the liquid phase was performed using the Calphad Optimizer module, constrained by this experimental evidence. The optimised interaction parameters are reported in Table 3. The calculated phase diagram and its comparison with the experimental data are shown in Fig. 6. Overall, the optimised thermodynamic description provides a satisfactory reproduction of the phase equilibria. The predicted phases at 69.2 mol% of $CaSO_4$ corresponded to those identified by XRD (Fig. S4, Table S7): MCl_2 phase containing mainly $CaCl_2$, $CaMg_2(SO_4)_3$, and $CaSO_4$. Additionally, calorimetric measurements on the $MgCl_2$(78.34 mol%)-$CaSO_4$(21.66 mol%) mixture were used to further evaluate the reliability of the thermodynamic model. At that composition, two phase transitions are observed: $CaCl_2 + MgCl_2 + CaMg_2(SO_4)_3 \rightleftharpoons$ Liquid + $MgCl_2 + CaMg_2(SO_4)_3$ at 577.8 °C and Liquid + $MgCl_2 + CaMg_2(SO_4)_3 \rightleftharpoons$ Liquid at 621.7 °C. The calculated minimum in the liquidus is at 20.4 mol% $CaSO_4$. Fig. S5 presents the comparison between the experimentally determined enthalpy increments as a function of temperature and those calculated from the developed database, as well as from the commercial database FTsalt [19]. The experimental enthalpy increments were obtained by integration of the measured heat capacity curves (Fig. 5). The observed agreement between experimental and calculated data supports the consistency and predictive capability of the

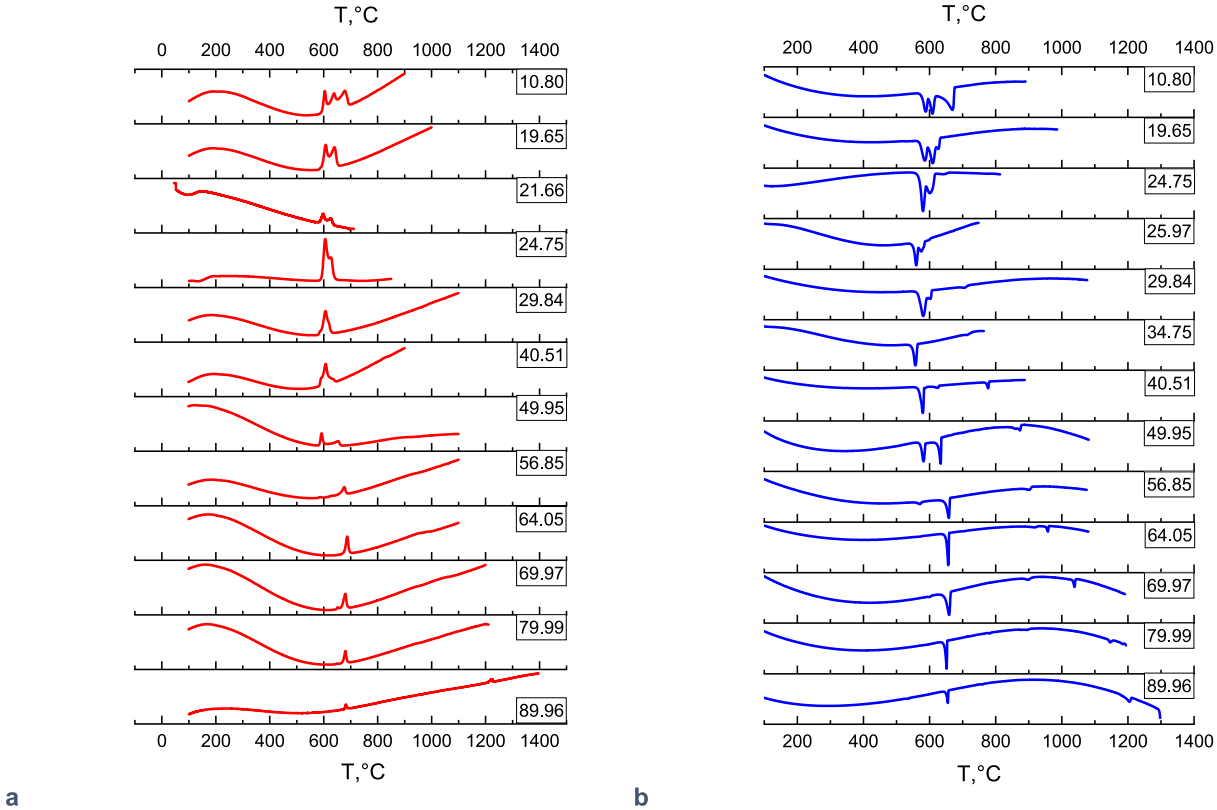

Fig. 4. DTA curves of $MgCl_2$-$CaSO_4$ mixtures, expressed in molar percentage of $CaSO_4$: **a** heating curves; **b** cooling curves.

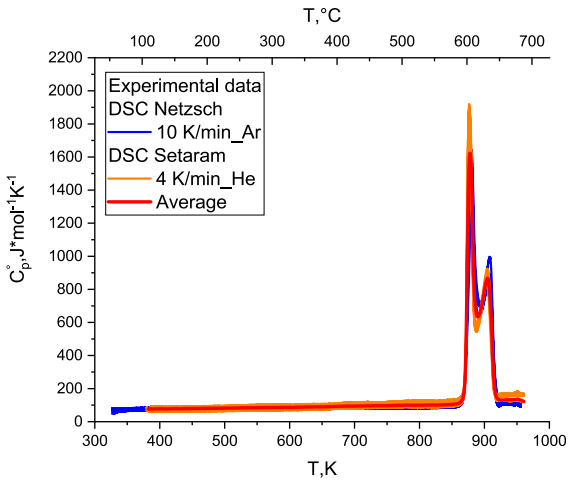

Fig. 5. Experimental values of molar heat capacity of $MgCl_2$(78.34 mol %)-$CaSO_4$(21.66 mol%).

optimised thermodynamic parameters.

4.3. $CaCl_2$-$MgSO_4$

A series of fifteen mixtures, covering the full compositional range were investigated by DTA. These experiments were conducted in sealed platinum tubes, and no mass loss was observed up to 1300 °C. The corresponding DTA heating and cooling curves for these mixtures are presented in Fig. 7, while the corresponding transition temperatures are summarised in Table S8.

A selected mixture with the composition $CaCl_2$(71.70 mol %)-$MgSO_4$(28.30 mol%) was prepared *in situ* and analysed by XRD in order to investigate the potential presence of intermediate compounds and better understand the phase equilibria in the system. The mixture was synthesised following the standard protocol: the pure compounds were mixed in their appropriate stoichiometric ratio, sealed within an evacuated quartz ampoule, and subjected to heat treatment, in this case at 900 °C for 60 h in a furnace. The resulting diffraction pattern measured at room temperature are summarised in Fig. S6 and Table S9. They indicate the presence of $CaCl_2$ and $CaMg_2(SO_4)_3$ as the main crystalline phases. This finding provides additional evidence regarding the phase fields within the corresponding regions of the phase diagram. Furthermore, the test confirmed the absence of other multicomponent chloride-sulphate phases.

4.3.1. *Thermodynamic assessment*

For the $CaCl_2$-$MgSO_4$ binary system, the thermodynamic optimisation was carried out based on the phase equilibria information acquired in this work. The experimentally determined phase transition temperatures were adopted as the basis for the modelling of the liquid phase within the Optimizer module. The interaction parameters obtained from the optimisation are summarised in Table 3. The calculated phase diagram is shown in Fig. 8, together with the experimental data points. The resulting thermodynamic description provides a coherent representation of the system's phase behaviour.

4.4. $MgCl_2$-$CaMg_2(SO_4)_3$

The presence of the intermediate compound $CaMg_2(SO_4)_3$ within the binary system $MgSO_4$-$CaSO_4$ provided the opportunity to study two additional sections with chlorides, which were previously unexplored. This compound was identified and characterised by the authors in a recent study [3]. The mixtures in the system $MgCl_2$-$CaMg_2(SO_4)_3$ intended to be studied were prepared by directly mixing the end-members of the binary systems or equivalently by mixing the three pure compounds involved in the appropriate molar ratios. Interestingly, the high-sulphate mixtures in the system $MgCl_2$-$CaMg_2(SO_4)_3$ showed a mass loss at temperatures above 1200 °C when prepared by directly mixing the pure compounds ($MgCl_2$, $MgSO_4$, $CaSO_4$), whereas they showed no mass loss when the same mixtures were prepared by mixing the two end-members. Ten mixtures have been investigated in DTA/TG in sealed platinum tubes, and the transition temperatures are listed in Table S 10. The DTA heating and cooling curves for the mixtures under study are displayed in Fig. 9. Thermal events were clearly evident during both heating and cooling. In mixtures with a high content of the double sulphate, the thermal events during heating appeared less intense, whereas the crystallisation peaks observed during cooling were more pronounced. Nevertheless, the liquidus temperatures were determined based on the heating curves.

Based on the thermodynamic database updated through the modelling of the subsystems constituting the reciprocal system, for which the

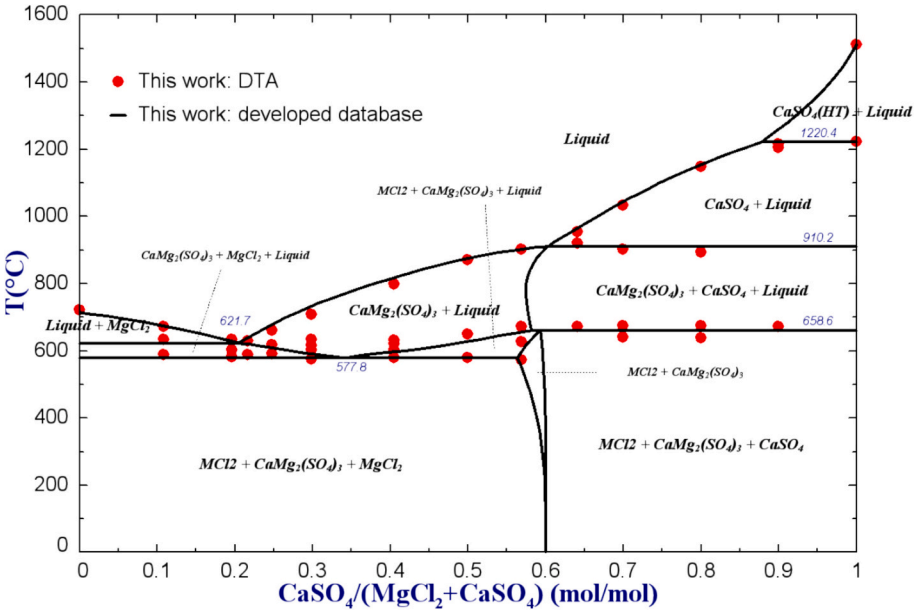

Fig. 6. Phase diagram of the $MgCl_2$-$CaSO_4$ system: comparison of experimental data obtained by DTA in the present work and calculation with the current database.

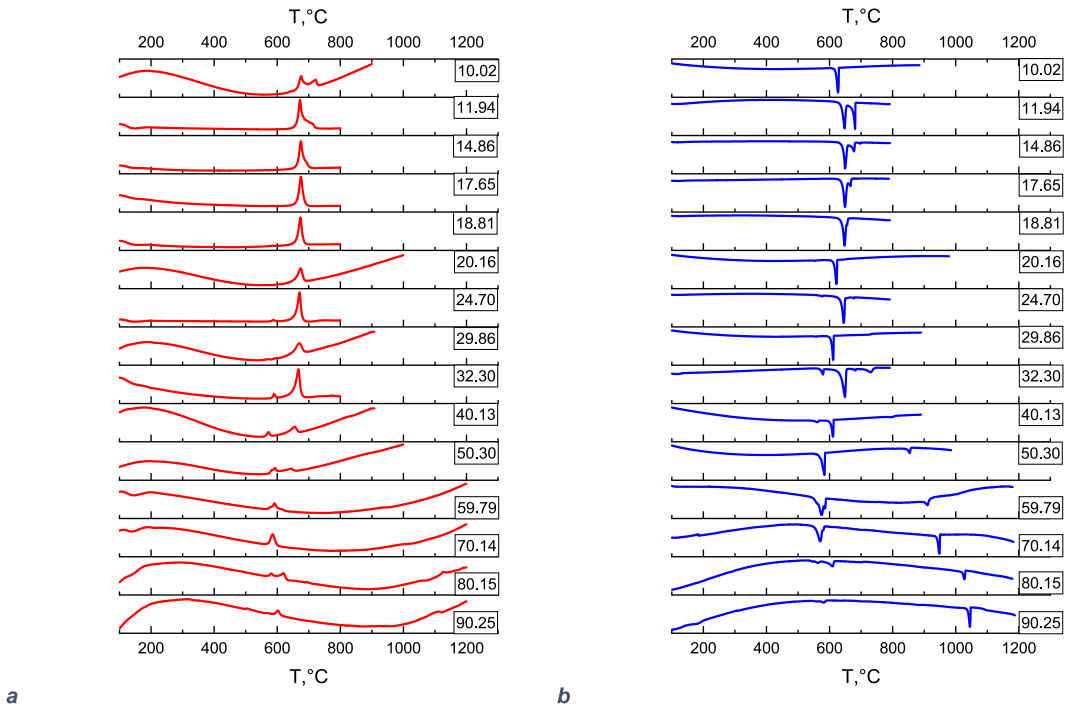

Fig. 7. DTA curves of $CaCl_2$-$MgSO_4$ mixtures, expressed in molar percentage of $MgSO_4$: **a** heating curves; **b** cooling curves.

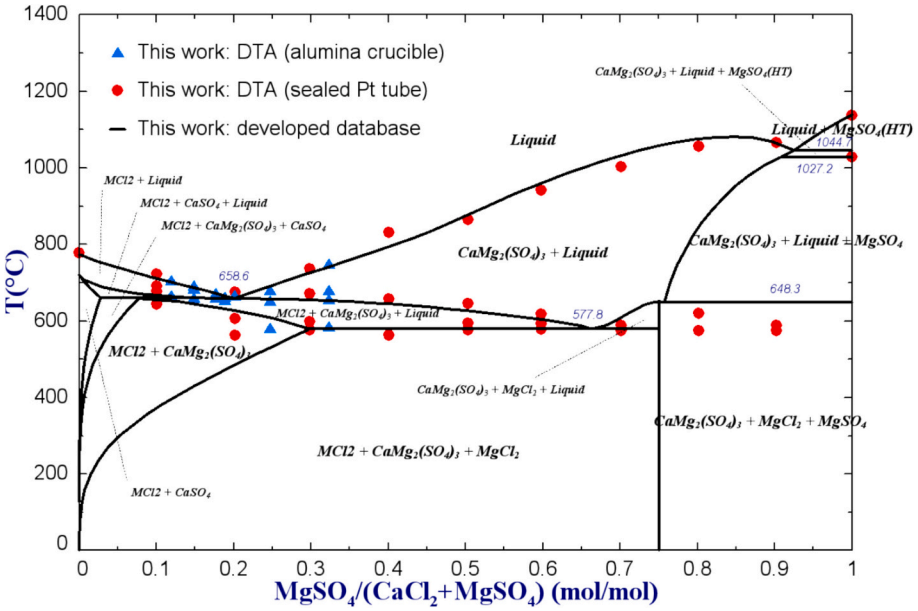

Fig. 8. Phase diagram of the $CaCl_2$-$MgSO_4$ system: comparison of experimental data obtained by DTA in the present work and calculation with the current database.

interaction parameters are reported in Table 3, the phase diagram of the $MgCl_2$-$CaMg_2(SO_4)_3$ section was calculated. Fig. 10 compares the experimental DTA data obtained in the present work with the phase diagram calculated using the developed database. The calculated diagram provides a good overall description of the experimental observations, in particular with respect to the liquidus curve and the eutectic equilibrium, which is predicted at 9.7 mol% $CaMg_2(SO_4)_3$ and a temperature of 659.5 °C. The calculated phase diagram does not reproduce a thermal effect observed experimentally at approximately 590 °C (see Table S 11). On the basis of the available experimental evidence, however, no additional phase can be unambiguously identified, and therefore no further phase equilibria can be conclusively established for this system. This isolated discrepancy is therefore considered to fall beyond the scope of the present thermodynamic description and is identified as a subject for future, targeted investigations. Importantly, it does not compromise the overall consistency of the database developed in this work, nor the reliability of the experimental data supporting the main phase relations of the system, which are reported here for the first time.

4.5. $CaCl_2$-$CaMg_2(SO_4)_3$

Nine mixtures have been investigated in DTA/TG in sealed platinum tubes. Their transition temperatures are listed in Table S 9 and their corresponding DTA curves are displayed in Fig. 11. Thermal events were

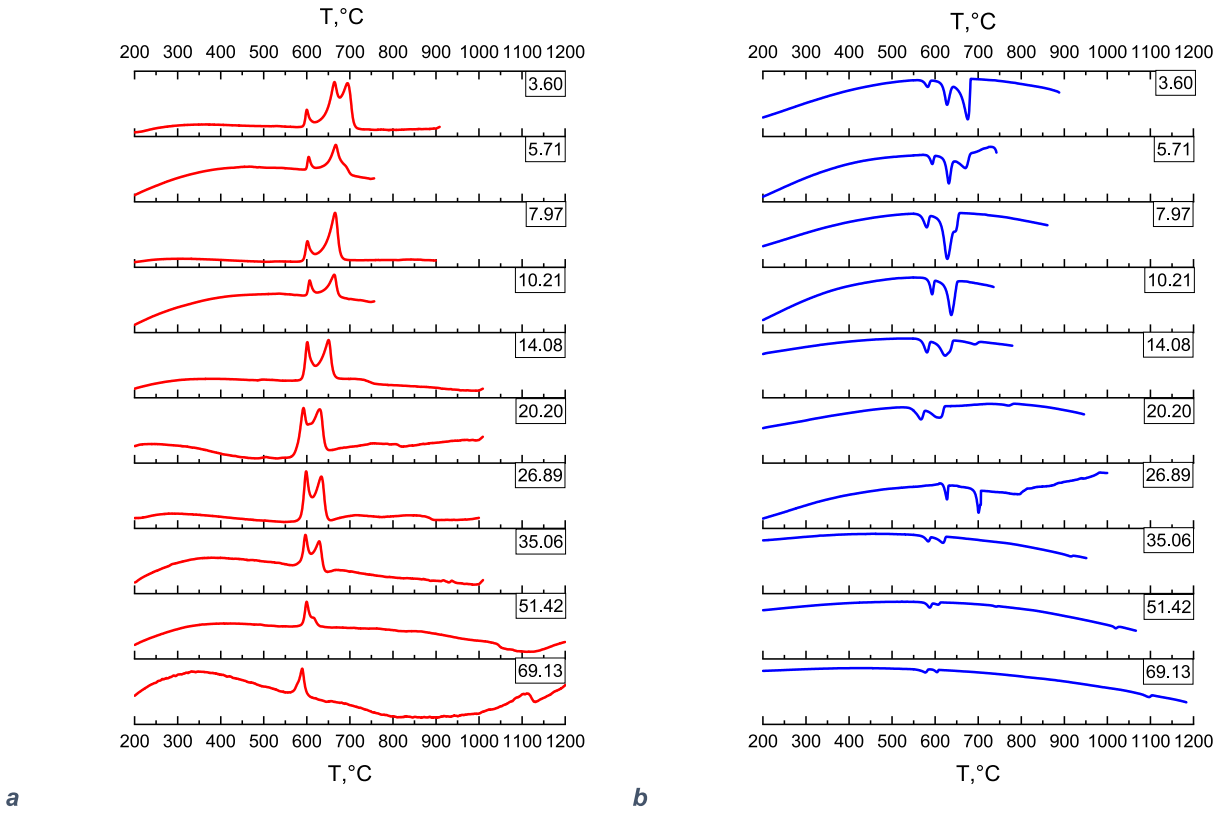

Fig. 9. DTA curves of $MgCl_2$-$CaMg_2(SO_4)_3$ mixtures, expressed in molar percentage of $CaMg_2(SO_4)_3$: **a** heating curves; **b** cooling curves.

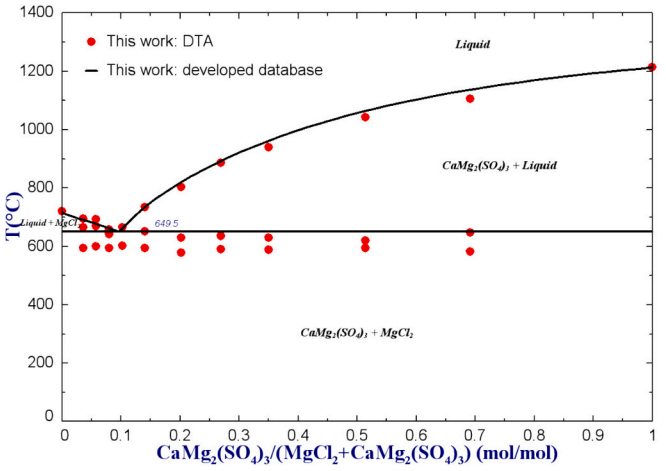

Fig. 10. Phase diagram of the $MgCl_2$-$CaMg_2(SO_4)_3$ system: comparison of experimental data obtained by DTA in the present work and calculation with the current database.

clearly evident during both heating and cooling. For mixtures with a high content of the double sulphate, these events appeared less intense, while the crystallisation observed during cooling remained more pronounced and provided clearer indications for detecting the liquidus temperature. The DTA measurements revealed several thermal effects, pointing to complex phase equilibria involving multiple phases and transitions. These effects, observed in both heating and cooling runs, together with the results discussed in the previous section, provide the first experimental evidence of the phase relations in the reciprocal system.

The phase diagram of the $CaCl_2$-$CaMg_2(SO_4)_3$ section was calculated on the basis of the thermodynamic database developed in this work from the assessment of the subsystems constituting the reciprocal system (see Table 3). The calculated phase diagram provides a good description of the phase equilibria identified experimentally, as shown in Fig. 12, with overall good agreement between calculation and experiment.

4.6. Mg^{2+}, Ca^{2+} // Cl^-, SO_4^{2-} system

The thermodynamic assessment of the reciprocal system was carried out by integrating the experimental data acquired in the present work with previously published results by the same authors on related binary systems [3,4], as well as additional data available in the literature. The Gibbs energy datasets on three binaries ($MgSO_4$-$CaSO_4$, $MgCl_2$-$MgSO_4$, and $CaCl_2$-$CaSO_4$) were generated in the previous work and kept constant, whereas the assessment of the fourth binary system, $MgCl_2$-$CaCl_2$, was performed in the present work. In the reciprocal system, the optimisation procedure was primarily based on the existing thermodynamic description of four key binary systems and on optimisation of the interaction parameters in the liquid to represent phase equilibria in all sections and the enthalpy increment in $MgCl_2$-$CaSO_4$. Phase equilibria data in two diagonal sections, $MgCl_2$-$CaSO_4$ and $CaCl_2$-$MgSO_4$ and two additional sections $CaCl_2$-$CaMg_2(SO_4)_3$ and $MgCl_2$-$CaMg_2(SO_4)_3$, were considered optimising the interactions between $MgCl_2$ and $CaSO_4$ as well as between $CaCl_2$ and $MgSO_4$. All optimised parameters are collected in Table 3. The experimental investigations on the $MgCl_2$-$CaMg_2(SO_4)_3$ and $CaCl_2$-$CaMg_2(SO_4)_3$ sections served as an additional validation tool for the thermodynamic database, allowing a direct comparison between the optimised database - resulting from the assessment of the six considered systems - and independent experimental findings.

Upon completion and validation of the thermodynamic optimisation of the binary sub-systems, the reciprocal system was subsequently modelled. The calculated phase diagram, reporting the liquidus projections, is presented in Fig. 13. There are eight primary crystallisation fields in the phase diagram, four of which correspond to pure sulphates,

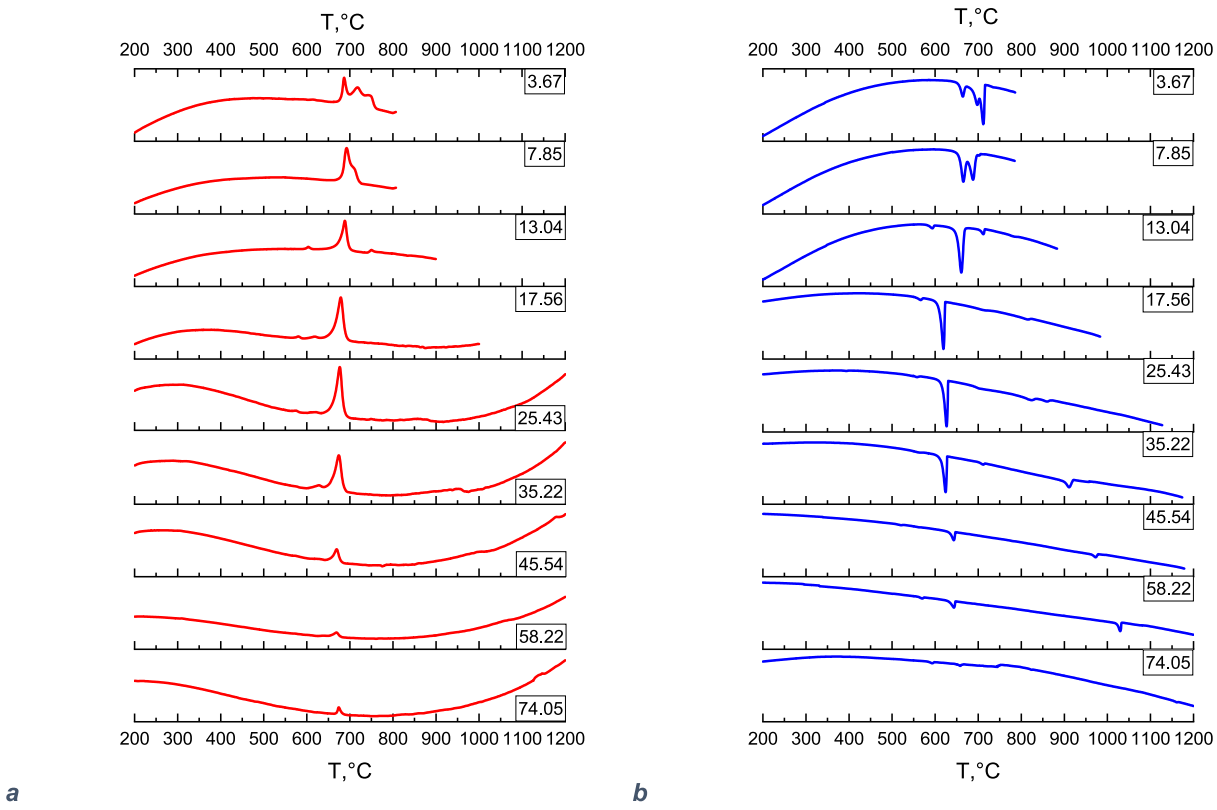

Fig. 11. DTA curves of $CaCl_2$-$CaMg_2(SO_4)_3$ mixtures, expressed in molar percentage of $CaMg_2(SO_4)_3$: **a** heating curves; **b** cooling curves.

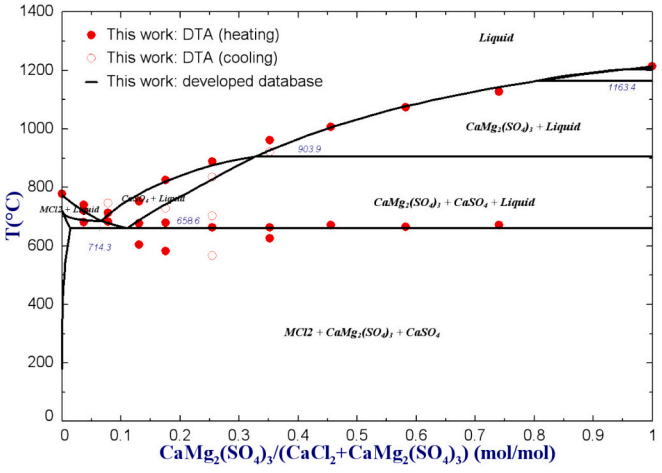

Fig. 12. Phase diagram of the $CaCl_2$-$CaMg_2(SO_4)_3$ system: comparison of experimental data obtained by DTA in the present work and calculation with the current database.

other two to pure $MgCl_2$ and the solid solution phase based on $CaCl_2$ (MCl2), and the remaining two to double magnesium-calcium sulphates. According to the generated dataset, the minimum temperature on the liquidus surface is calculated at 578 °C (851 K). The diagram highlights several minima in the liquidus projections, corresponding to possible eutectic compositions (Table 2), which may represent potential candidates for experimental verification and application as phase change materials, and which may be investigated in a follow-up study to further validate the thermodynamic database and assess their suitability for thermal energy storage. Among these, two invariant points, denoted as P4 and P5 in Table 2, appear particularly relevant, as they exhibit comparatively high enthalpy values associated with the fusion transition. Expressed in terms of independent components, P4 corresponds to the ternary composition $MgCl_2$(73.14 mol%)-$MgSO_4$(20.75 mol%)-$CaSO_4$(6.11 mol%), with a melting temperature of 648 °C (921 K) and a fusion enthalpy of 42 kJ/mol, whereas P5 corresponds to the composition $MgCl_2$(65.61 mol%)-$CaCl_2$(15.51 mol%)-$CaSO_4$(18.88 mol %), melting at 578 °C (851 K) with an associated enthalpy of 34.5 kJ/mol. These compositions therefore emerge from the present thermodynamic screening as attractive candidates for further experimental investigation in the context of inorganic PCM applications.

5. Conclusions

This work presented the continuation and consolidation of an experimental campaign initiated in previous studies on binary systems, aimed at the thermodynamic assessment of the Mg^{2+}, Ca^{2+} // Cl^-, SO_4^{2-} reciprocal system. The experimental investigation combined thermal and calorimetric analyses, specifically Differential Thermal Analysis coupled with Thermal Gravimetry (DTA/TG), and Differential Scanning Calorimetry (DSC), supported, where necessary, by crystallographic characterisation. The experimental findings in the system $MgCl_2$-$CaCl_2$ and various sections in the reciprocal system enabled the clarification of phase equilibria and the construction of the phase diagrams of the systems under investigation. These results provided a consistent and reliable dataset for the subsequent thermodynamic assessment and modelling of the reciprocal system. The present work provided thermodynamic data for the eutectic mixture $MgCl_2$(52.81 mol %)-$CaCl_2$(47.19 mol%), which exhibits a melting temperature of 624 °C (897 K) and an associated latent heat of fusion of 33.2 ± 0.8 kJ/mol. Using the FactSage software package, the interaction parameters in the liquid phase were optimised to reproduce the phase equilibria and enthalpy increment in the reciprocal system. The integrated approach adopted in this study – combining newly acquired experimental data with information previously obtained on pure compounds and binary subsystems - allowed the extension and improvement of the

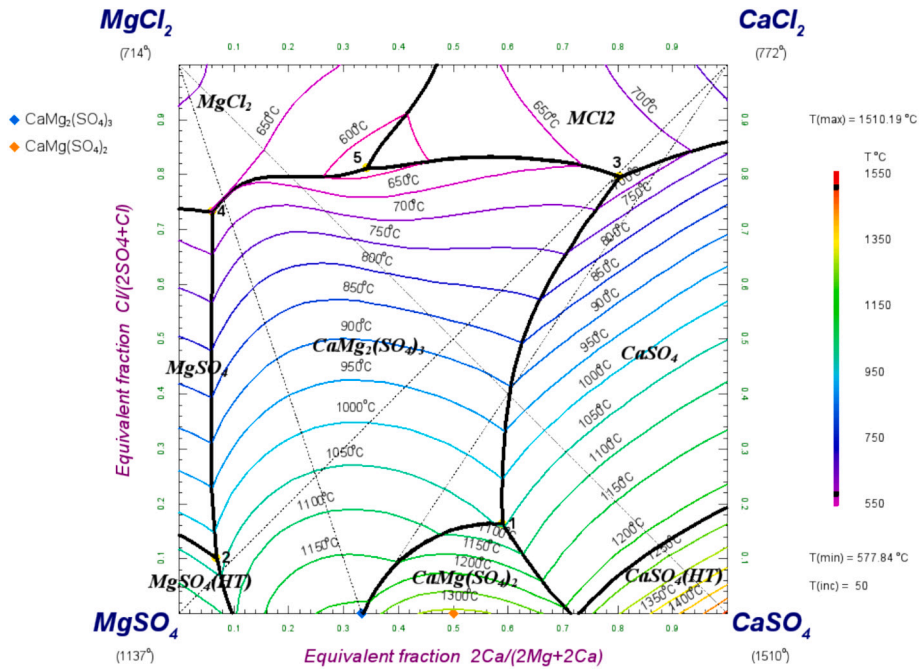

Fig. 13. Liquidus surface of the reciprocal system Mg^{2+}, Ca^{2+} // Cl^-, SO_4^{2-} calculated with the current database.

Table 2
Calculated invariant points in the reciprocal system Mg^{2+}, Ca^{2+} // Cl^-, SO_4^{2-}.

	$\frac{2Ca}{2Mg+2Ca}$	$\frac{Cl}{2SO_4+Cl}$	T, °C	Solid phase
P1	0.5910	0.1624	1044.2	$CaSO_4$, $CaMg(SO_4)_2$, $CaMg_2(SO_4)_3$
P2	0.0690	0.1005	1027.2	$MgSO_4$(LT), $MgSO_4$(HT), $CaMg_2(SO_4)_3$
P3	0.8045	0.7955	658.6	MCl2, $CaSO_4$, $CaMg_2(SO_4)_3$
P4	0.0612	0.7314	648.3	$MgCl_2$, $MgSO_4$(LT), $CaMg_2(SO_4)_3$
P5	0.3438	0.8113	577.8	$MgCl_2$, MCl2, $CaMg_2(SO_4)_3$

LT: low-temperature phase modification; HT: high-temperature phase modification; MCl2: solid solution $(Mg^{2+}, Ca^{2+})_1(Cl^-)_2$.

thermodynamic database. The optimised dataset now offers an accurate and internally consistent description of the thermodynamic behaviour of chloride-sulphate systems containing alkaline-earth metals, providing a solid basis for future investigations and potential technological applications. Within this context, the eutectic composition in the binary system $MgCl_2$-$CaCl_2$ can be regarded as a thermodynamically suitable candidate for phase change material applications. In contrast, the experimentally characterised low-melting mixture $MgCl_2$(78.34 mol %)-$CaSO_4$(21.66 mol%) does not represent a thermodynamically optimal PCM candidate. This is due to the proximity of two distinct thermal events, which would complicate the charging and discharging processes in practical applications. Two multicomponent compositions in the reciprocal system further emerge as thermodynamically promising. Expressed in terms of independent components, these correspond to $MgCl_2$(73.14 mol%)-$MgSO_4$(20.75 mol%)-$CaSO_4$(6.11 mol%), exhibiting a melting temperature of 648 °C (921 K) and a fusion enthalpy of 42 kJ/mol, and $MgCl_2$(65.61 mol%)-$CaCl_2$(15.51 mol %)-$CaSO_4$(18.88 mol%), with a melting temperature of 578 °C (851 K) and an associated enthalpy of 34.5 kJ/mol.

CRediT authorship contribution statement

Amedeo Morsa: Writing – review & editing, Writing – original draft, Visualization, Validation, Software, Methodology, Investigation, Formal analysis, Data curation, Conceptualization. **Elena Yazhenskikh:** Writing – review & editing, Writing – original draft, Visualization, Validation, Supervision, Software, Methodology, Formal analysis, Data curation, Conceptualization. **Rhys Dominic Jacob:** Writing – review & editing, Visualization, Validation. **Michael Müller:** Writing – review & editing, Visualization, Validation, Supervision, Software, Resources,

Table 3
Thermodynamic descriptions of the liquid and solid solution phases.

Gibbs energy data, J/mol	Ref.
Liquid: ($MgCl_2$/1.5, $MgSO_4$, $CaCl_2$/1.5, $CaSO_4$)	
${}^{\circ}G_{MgCl_2} = {}^{\circ}G_{MgCl_2(liquid)}$	[29]
${}^{\circ}G_{MgSO_4} = {}^{\circ}G_{MgSO_4(liquid)}$	[3]
${}^{\circ}G_{CaCl_2} = {}^{\circ}G_{CaCl_2(liquid)}$	[30]
${}^{\circ}G_{CaSO_4} = {}^{\circ}G_{CaSO_4(liquid)}$	[31]
$L^{(0)}_{CaCl_2,MgCl_2} = 1294.86 + 7.71978*T$	a
$L^{(1)}_{CaCl_2,MgCl_2} = -2221.13 + 1.70498*T$	a
$L^{(0)}_{CaSO_4,MgSO_4} = -10697.8 + 0.93*T$	[3]
$L^{(1)}_{CaSO_4,MgSO_4} = 5791.59 + 4.94*T$	[3]
$L^{(2)}_{CaSO_4,MgSO_4} = 2192.44$	[3]
$L^{(0)}_{MgSO_4,MgCl_2} = -27772.3 + 18*T$	[4]
$L^{(1)}_{MgSO_4,MgCl_2} = -2606.47 - 4.89221*T$	[4]
$L^{(0)}_{CaCl_2,CaSO_4} = 35970.8 - 21.371*T$	[4]
$L^{(1)}_{CaCl_2,CaSO_4} = -5159.39 - 1.5534*T$	[4]
$L^{(0)}_{CaSO_4,MgCl_2} = -12262 + 6*T$	a
$L^{(1)}_{CaSO_4,MgCl_2} = 20600$	a
$L^{(0)}_{CaCl_2,MgSO_4} = -13000$	a
MCl2: $(Mg^{2+}, Ca^{2+})_1(Cl^-)_2$	
${}^{\circ}G_{MgCl_2} = {}^{\circ}G_{MgCl_2(liquid)} + 29550.2 - 18.4261$	[18]
${}^{\circ}G_{CaCl_2} = {}^{\circ}G_{CaCl_2(liquid)}$	[18]

[a] This work.

Project administration, Methodology, Funding acquisition, Conceptualization. **Dmitry Sergeev:** Writing – review & editing, Visualization, Validation, Supervision, Resources, Project administration, Methodology, Funding acquisition, Conceptualization.

Declaration of competing interest

The authors declare that they have no known competing financial interests or personal relationships that could have appeared to influence the work reported in this paper.

Acknowledgements

This work was supported by the Federal Ministry for Economic Affairs and Climate Action on the basis of a decision by the German Bundestag within the project PCM-Screening 2 (FKZ 03EN6005D). Acknowledgment is extended to Mirko Ziegner for assistance with the XRD analyses (see Supplementary Information).

Appendix A. Supplementary data

Supplementary data to this article can be found online at https://doi.org/10.1016/j.jct.2026.107681.

Data availability

Data will be made available on request.

References

[1] M.M. Kenisarin, High-temperature phase change materials for thermal energy storage, Renew. Sustain. Energy Rev. 14 (3) (2010) 955–970.
[2] B. Cárdenas, N. León, High temperature latent heat thermal energy storage: phase change materials, design considerations and performance enhancement techniques, Renew. Sustain. Energy Rev. 27 (2013) 724–737.
[3] A. Morsa, E. Yazhenskikh, M. Ziegner, E. Wessel, R.D. Jacob, M. Müller, D. Sergeev, Experimental study and thermodynamic assessment of the $MgSO_4$-$CaSO_4$ system, Calphad 90 (2025) 102855.
[4] A. Morsa, E. Yazhenskikh, R.D. Jacob, M. Müller, D. Sergeev, Thermodynamics of the $MgCl_2$-$MgSO_4$ and $CaCl_2$-$CaSO_4$ systems, Calphad 91 (2025) 102888.
[5] J. Rowe, G. Morey, I. Hansen, The binary system K_2SO_4-$CaSO_4$, J. Inorg. Nucl. Chem. 27 (1965) 53–58.
[6] R. Nacken, Ueber Langbeinit und Vanthoffit (K_2SO_4. $2MgSO_4$ und $3Na_2SO_4$. $MgSO_4$), Nachrichten von der Gesellschaft der Wissenschaften zu Göttingen, Math.-Phys. Kl. 1907 (1907) 602–613.
[7] A. Ginsberg, Über die verbindungen von magnesium-und natriumsulfat, Z. Anorg. Chem. 61 (1) (1909) 122–136.
[8] J. Rowe, G. Morey, C. Silber, The ternary system K_2SO_4•$MgSO_4$•$CaSO_4$, J. Inorg. Nucl. Chem. 29 (1967) 925–942.
[9] A. Abhat, Low temperature latent heat thermal energy storage: heat storage materials, Sol. Energy 30 (1983) 313–332.
[10] A.S.F.T. Materials, Standard test method for determining specific heat capacity by differential scanning calorimetry, ASTM International, 2011.
[11] D. Ditmars, S. Ishihara, S. Chang, G. Bernstein, E. West, Enthalpy and heat-capacity standard reference material: synthetic sapphire (α-Al2O3) from 10 to 2250 k, J. Res. Natl. Bur. Stand. 87 (2) (1982) 159.
[12] K. Hack, The SGTE casebook: thermodynamics at work, Elsevier, 2008.
[13] T.M. Besmann, K.E. Spear, Thermochemical modeling of oxide glasses, J. Am. Ceram. Soc. 85 (12) (2002) 2887–2894.
[14] E. Yazhenskikh, K. Hack, M. Müller, Critical thermodynamic evaluation of oxide systems relevant to fuel ashes and slags. Part 1: alkali oxide–silica systems, Calphad 30 (3) (2006) 270–276.
[15] J. Qi, E. Yazhenskikh, M. Ziegner, X. Zhao, G. Wu, M. Müller, D. Sergeev, Experimental study and thermochemical assessment of the reciprocal system li^+, K^+//Cl^-, CO_3^{2-}, Calphad 83 (2023) 102603.
[16] Database GTOx, GTT-Technologies, forschungszentrum jülich, 2010–2025, GTT-Technologies.
[17] B. Sundman, J. Ågren, A regular solution model for phases with several components and sublattices, suitable for computer applications, J. Phys. Chem. Solid 42 (4) (1981) 297–301.
[18] P. Chartrand, A.D. Pelton, Thermodynamic evaluation and optimization of the LiCl-NaCl-KCl-RbCl-CsCl-$MgCl_2$-$CaCl_2$ system using the modified quasi-chemical model, Metall. Mater. Trans. A 32A (2001) 1361–1383.
[19] C.W. Bale, E. Bélisle, P. Chartrand, S.A. Decterov, G. Eriksson, A.E. Gheribi, K. Hack, I.H. Jung, Y.B. Kang, J. Melançon, A.D. Pelton, S. Petersen, C. Robelin, J. Sangster, P. Spencer, M.A. Van Ende, FactSage thermochemical software and databases, 2010–2016, Calphad 54 (2016) 35–53.
[20] FactSage, Facility for the Analysis of Chemical Thermodynamics, Version 8.3. Available from: http://www.factsage.com/.
[21] B. Reis, F. Tang, P. Keuter, M. Baben, User-friendly and robust calphad optimizations using calphad optimizer in FactSage, Calphad 88 (2025) 102800.
[22] O. Menge, Die binaren systeme von $MgCl_2$ und $CaCl_2$ mit den chloriden der metalle K, Na, Ag, Pb, Cu, Zn, Sn und Cd, Voss, 1911, pp. 162–218.
[23] A.I. Ivanov, Phase diagram of the system KCl-MgCl2-CaCl2 Izvest, Sektora Fiz.-Khim. Anal., Akad. Nauk S.S.S.R 23 (1953) 189–200.
[24] K. Matiašovský, Phase diagrams of some systems important in electrolytic production of magnesium. I. Two-component systems $MgCl_2$-NaCl, $CaCl_2$-NaCl, and $MgCl_2$-$CaCl_2$, Chem. Pap. 13 (2) (1959) 69–77.
[25] K. Grjotheim, J.L. Holm, J. Malmo, The phase diagram of the system MgCl2-CaCl2, and thermo-dynamic properties of molten mixtures in this system, Acta Chem. Scand. 24 (1970) 77–86.
[26] I. Karakaya, W.T. Thompson, Thermodynamic properties of {(1-x)$MgCl_2$+x$CaCl_2$} (l), J. Chem. Thermodyn. 18 (1986) 859–866.
[27] I. Karakaya, W.T. Thompson, A thermodynamic study of the system $MgCl_2$–NaCl–$CaCl_2$, Can. Metall. Quart. 25 (4) (1986) 307–317.
[28] A.D. Pelton, A database and sublattice model for molten salts, Calphad 12 (2) (1988) 127–142.
[29] https://www.enargus.de/pub/bscw.cgi/?op=enargus.eps2&q=PCM-2&v=10&id=2029269.
[30] B.H. Reis, Development of a novel thermodynamic database for salt systems with potential as phase change materials, BTU Cottbus-Senftenberg, 2021.
[31] E. Yazhenskikh, T. Jantzen, D. Kobertz, K. Hack, M. Müller, Critical thermodynamic evaluation of the binary sub-systems of the core sulphate system Na_2SO_4–K_2SO_4–$MgSO_4$–$CaSO_4$, Calphad 72 (2021) 102234.